Journal of Fluids and Structures (2002) **16**(2), 175–191
doi:10.1006/jfls.2001.0413, available online at http://www.idealibrary.com on IDEAL®

FLOW VISUALIZATION AROUND A CIRCULAR CYLINDER NEAR TO A PLANE WALL

S. J. Price, D. Sumner†, J. G. Smith, K. Leong and M. P. Païdoussis

Department of Mechanical Engineering, McGill University
Montreal, Québec, Canada H3A 2K6

(Received 21 October 1999, and in final form 20 April 2001)

Flow visualization, particle image velocimetry and hot-film anemometry have been employed to study the fluid flow around a circular cylinder near to a plane wall for Reynolds numbers, based on cylinder diameter, between 1200 and 4960. The effect of changing the gap between the cylinder and the wall, G, from $G = 0$ (cylinder touching the wall) to $G/D = 2$, was investigated. It is shown that the flow may be characterized by four distinct regions. (a) For very small gaps, $G/D \leq 0{\cdot}125$, the gap flow is suppressed or extremely weak, and separation of the boundary layer occurs both upstream and downstream of the cylinder. Although there is no regular vortex shedding, there is a periodicity associated with the outer shear-layer. (b) In the "small gap ratio" region, $0{\cdot}125 < G/D < 0{\cdot}5$, the flow is very similar to that for very small gaps, except that there is now a pronounced pairing between the inner shear-layer shed from the cylinder and the wall boundary layer. (c) Intermediate gap ratios, $0{\cdot}5 < G/D < 0{\cdot}75$, are characterized by the onset of vortex shedding from the cylinder. (d) For the fourth region, characterized by the largest gap ratios considered, $G/D > 1{\cdot}0$, there is no separation of the wall boundary layer, either upstream or downstream of the cylinder.

1. INTRODUCTION

There are many practical examples where cylindrical structures close to a solid surface are subjected to a transversely flowing fluid (shown schematically in Figure 1), pipelines on a seabed being one example. Although the fluid dynamics of an isolated circular cylinder in a steady flow is now reasonably well understood [for example, see Zdravkovich (1997)], this is not the case when the cylinder is positioned close to a plane wall boundary.

One of the first pieces of research in this area was by Taneda (1965), who presented flow visualization at a Reynolds number, based on cylinder diameter and towing velocity, of $\mathrm{Re} = 170$. The cylinder was towed through stagnant water close to a stationary wall; hence, there were no boundary layer effects. For a gap-to-diameter ratio, G/D, of 0·1 only a single row of vortices was shed from the cylinder, while for $G/D = 0{\cdot}6$ a regular double row of vortices was shed; a summary of this and all other work reviewed in this paper is presented in Table 1.

Bearman & Zdravkovich (1978) investigated the flow around a stationary cylinder close to a plane wall for higher Reynolds numbers, $\mathrm{Re} = 2{\cdot}5 \times 10^4$ and $4{\cdot}5 \times 10^4$. In these experiments a boundary layer developed on the wall. Hot-wire measurements were conducted for a turbulent boundary layer, and its thickness, δ, at the location of the cylinder, but

† Now with the Department of Mechanical Engineering, University of Saskatchewan, Saskatoon, Saskatchewan, Canada.

0889–9746/02/020175 + 17 $35.00/0

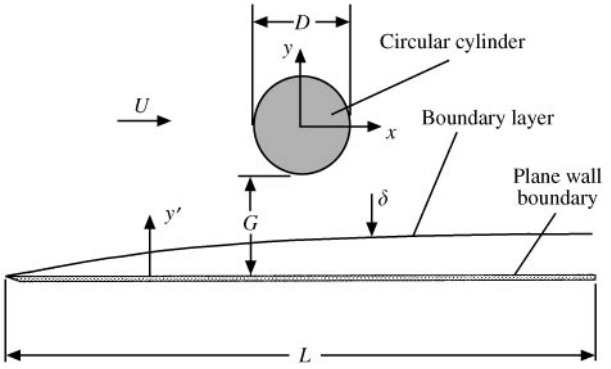

Figure 1. Schematic showing the cylinder and plane wall boundary.

with the cylinder removed, was 0·8D. For $G/D > 0{\cdot}3$, regular vortex shedding occurred, and the Strouhal number, St, was sensibly independent of G/D. On the other hand, regular vortex shedding was suppressed for $G/D < 0{\cdot}3$, although in some cases a weak vortex shedding signal was obtained near the edge of the cylinder farthest away from the wall. Pressure measurements showed that the effect of the wall was felt for $G/D < 1{\cdot}0$ approximately, and that for $G/D < 0{\cdot}6$ there was a rapid decrease in the magnitude of the base pressure coefficient as the gap was decreased. The pressure measurements also showed that, for small gaps, the front stagnation point was rotated towards the plane wall, resulting in a steady mean lift force repelling the cylinder away from the wall; this was in agreement with previous results by Roshko *et al.* (1975). Later, Zdravkovich (1985) showed that the cylinder drag is dominated by G/δ, and is sensibly unaffected by the gap to diameter ratio, G/D.

Flow visualization conducted by Bearman & Zdravkovich (1978) with a thinner boundary layer than that used for their hot-wire measurements suggested that vortex shedding was suppressed for small G/D. In addition, when vortex shedding was suppressed, separation bubbles formed both upstream and downstream of the cylinder on the plate. Zdravkovich (1980) continued work on the flow visualization for $\mathrm{Re} = 2{\cdot}5 \times 10^4$, and suggested that, when the cylinder was in contact with the wall, $G/D = 0$, upstream and downstream separation regions were attached to the cylinder, and that the downstream separation region contained two counter-rotating vortices separated by stagnant fluid. No regular vortex shedding was observed for this configuration. As G/D was increased, regular vortex shedding resumed at $G/D = 0{\cdot}2$ in the wind tunnel (turbulent boundary layer) and $G/D = 0{\cdot}4$ in the smoke tunnel (laminar boundary layer). A strong gap flow and the disappearance of the upstream separation bubble accompanied the resumption of regular vortex shedding.

In later experiments, Zdravkovich (1983) studied the flow around a cylinder towed close to a wall (hence, there were no boundary layer effects) at $\mathrm{Re} = 3{\cdot}55 \times 10^3$. For $G/D = 0{\cdot}1$ and 0·3, a single row of erratic and irregular vortices formed on the cylinder surface away from the wall. For $0{\cdot}3 \leq G/D \leq 0{\cdot}6$, a regular vortex street was shed from the side of the cylinder away from the wall, with separation "humps" forming on the wall between vortices shed from the other side of the cylinder. For $G/D > 0{\cdot}6$, regular alternate vortex shedding was observed.

Buresti & Lanciotti (1979) also investigated the effect of G/D on the vortex shedding frequency, but in a higher range of Reynolds numbers ($0{\cdot}86 \times 10^5$–$3{\cdot}0 \times 10^5$) and for a much thinner boundary layer ($\delta = 0{\cdot}1D$). For a smooth cylinder, the critical gap below which vortex shedding did not occur was between 0·3 and 0·4D; however, for a roughened cylinder

TABLE 1

Summary of previous work for flow around a circular cylinder close to a plane wall. Experimental set-up: "A", flow over a stationary cylinder next to a stationary plane wall; "B", cylinder towed through fluid next to the stationary plane wall. Type of measurements: "FV", flow visualization; "HW", hot-wire and/or hot-film measurements of vortex shedding frequencies; "SW", stop-watch measurements of vortex-shedding frequencies; "PM", pressure measurements on cylinder; "FM", force measurements on cylinder; "VM" velocity traverses of the cylinder wake

	Re	G/D	δ/D	Exp. set-up	Type of measurement	Critical G/D to suppress vortex shedding	Other effects of G/D
Taneda (1965)	170	0·1, 0·6	—	B	FV	—	—
Roshko *et al.* (1975)	2×10^4	0·0–6·0	0·5	A	FM	—	Max. C_D at $G/D = 0{\cdot}6$
Bearman & Zdravkovich (1978)	$2{\cdot}5 \times 10^4$ and $4{\cdot}5 \times 10^4$	0·0–3·5	0·8 for PM and HF; $<0{\cdot}8$ for FV	A	PM, HF, FV	0·3	St almost independent of G/D
Buresti & Lanciotti (1979)	$0{\cdot}85 \times 10^5$–$3{\cdot}0 \times 10^5$	0·0–2·5	0·1	A	HF	0·3–0·4 for smooth cylinder 0·2–0·3 for rough cylinder	No effect of wall for $G/D > 0{\cdot}4$
Zdravkovich (1980)	$2{\cdot}5 \times 10^4$	0·0–2·0	—	A	FV	0·2 and 0·4 for turbulent and laminar boundary layer	—
Angrilli *et al.* (1982)	2860, 3820 and 7640	0·5–6·0	$\leq 0{\cdot}25$	A	FV, VM	—	St increases as G/D decreases, to max. at $G/D = 0{\cdot}5$
Zdravkovich (1983)	3550	0·1–1·6	—	B	FV	0·3	No effect of wall for $G/D > 1{\cdot}4$
Grass *et al.* (1984)	1785 and 3570	0·0–2·0	0·28, 2·6 and 6·0	A	FV, HF, VM	0·3	St increases as G/D decreases, to max. at $G/D = 0{\cdot}75$ and 0·5 for $\delta/D = 0{\cdot}28$ and 6 St independent of δ/D
Zdravkovich (1985)	$4{\cdot}8 \times 10^4$–$3{\cdot}0 \times 10^5$	0·0–2·0	0·12–0·97	A	FM	—	C_D independent of G/D, C_L very dependent on G/D
Taniguchi & Miyakoshi (1990)	$9{\cdot}4 \times 10^4$	0·0–3·0	0·34–1·05	A	HF, FM, PM, FV	0·3 at $\delta/D = 0{\cdot}34$ 0·9 at $\delta/D = 1{\cdot}05$	No variation in St for $G/D >$ critical value
Cheng *et al.* (1994)	500	0·0–5·0	$< 1{\cdot}0$	A	FV, SW	0·125	Maximum St at $G/D = 0{\cdot}625$
Lei *et al.* (1999)	1.3×10^4	0·0–3·0	0·14–2·89	A	PM	0·2–0·3	C_D affected more by G/D than δ/D

(said to produce supercritical flow for an isolated cylinder), the critical gap was between 0·2 and 0·3D. For gaps greater than the critical values, St was independent of G/D.

Angrilli *et al.* (1982) investigated the effect of G/D on the vortex shedding frequency in a much lower range of Re (2860, 3820 and 7640). Contrary to previous experiments, they found that for $G/D < 5{\cdot}0$ the gap ratio had a fairly strong effect on St. For example, at $G/D = 0{\cdot}5$ (the minimum value they tested) St was 10% greater than that at $G/D = 5{\cdot}0$. As discussed by Angrilli *et al.*, a possible reason for the difference between their results and those of Buresti & Lanciotti (1979) and Bearman & Zdravkovich (1978) is the difference in Re.

Grass *et al.* (1984) investigated the vortex shedding response behind a cylinder with three different boundary-layer thicknesses, $\delta/D \approx 0{\cdot}28$, 2·6 and 6·0, for two different Reynolds numbers, Re = 1785 and 3570. Unfortunately, they defined St with respect to the local velocity, not the free-stream velocity as is more conventional; hence, it is difficult to compare their values of St with those obtained by others. However, their variation of St with G/D was reasonably independent of δ, and there was a gradual increase in St as G/D was decreased below 2·0. For $\delta/D = 0{\cdot}28$, the maximum St, which occurred at $G/D = 0{\cdot}75$, was 5–10% greater than that for large G/D; no vortex shedding was obtained for $G/D < 0{\cdot}3$. For the thick boundary layer, $\delta/D \approx 6$, the maximum St, occurring at $G/D = 0{\cdot}5$, was approximately 25% above the free-stream value, and no vortex shedding was obtained below this value of G/D. Grass *et al.* also noted that separation bubbles formed upstream and downstream of the cylinder for $\delta/D \approx 0{\cdot}28$ only, and not for the thicker boundary layers. It was suggested that the downstream separation produced a free jet, which caused a cancellation of vorticity on the side of the cylinder wake close to the wall, and hence eliminated the vortex shedding.

Taniguchi & Miyakoshi (1990) also considered the effect of boundary layer thickness at $\mathrm{Re} = 9{\cdot}4 \times 10^4$. They used trip wires to obtain $0{\cdot}34 \leq \delta/D \leq 1{\cdot}05$, and measured force coefficients on the cylinder as well as the vortex shedding frequency. The minimum G/D required to suppress vortex shedding increased with δ; for example, at $\delta/D = 0{\cdot}34$ and 1·05 the critical values of G/D were 0·3 and 0·9, respectively. However, independent of the value of δ, for G/D greater than the critical value, there was sensibly no variation in St with G/D. The critical G/D also corresponded to a local minimum in the fluctuating lift and drag coefficients. Using an argument similar to that given by Grass *et al.* (1984), Taniguchi and Miyakoshi suggested that the suppression of vortex shedding at small G/D is due to the cancellation of vorticity associated with the shear-layer on the wall and that shed from the cylinder.

Cheng *et al.* (1994) conducted flow visualization and vortex shedding frequency measurements, obtained by timing the vortex shedding via a stop-watch, for the flow around a cylinder close to a plane wall for Re = 500 and $0{\cdot}0 \leq G/D \leq 5{\cdot}0$. For $G/D < 1{\cdot}25$, they reported only a street of single vortices shed from the surface of the cylinder furthest away from the plane wall. They also observed the existence of both symmetric and antisymmetric vortex shedding for $G/D > 1{\cdot}25$, although the antisymmetric pattern was predominant. For $G/D \geq 2{\cdot}0$, the Strouhal number was constant at 0·2. However, for $G/D \leq 2{\cdot}0$, St increased as G/D decreased to a maximum of $\mathrm{St} = 0{\cdot}252$ at $G/D = 0{\cdot}625$; a further reduction in G/D causes St to decrease, till $\mathrm{St} = 0{\cdot}23$ is attained at $G/D = 0{\cdot}125$.

The effect of δ and G/D was also investigated by Lei *et al.* (1999) for $\mathrm{Re} \approx 1{\cdot}3 \times 10^4$. They created artificial boundary layers, giving $0{\cdot}14 \leq \delta/D \leq 2{\cdot}89$. The drag coefficient, C_D, was affected much more by varying G/D than by varying δ/D. For all δ/D, there was an almost linear increase in C_D with increasing G/D for $G/D \leq 0{\cdot}7$. Decreasing δ/D caused a slight increase in C_D. Lei *et al.* also suggested that a better way of determining whether or not vortex shedding occurs is to examine the r.m.s. of the fluctuating lift coefficient, a strong

signal implying that vortex shedding does occur. They showed that, as G/D is decreased below approximately 0·7, there is a rapid decrease in the r.m.s. lift, until it reaches a plateau at $G/D \approx 0{\cdot}2$–$0{\cdot}3$. It is this plateau region of low r.m.s. lift that they consider as representing no vortex shedding.

Kiya *et al.* (1980) examined the related problem of a circular cylinder in a shear flow. In particular, they measured St as a function of the "shear parameter" hD/U, where h is the transverse velocity gradient. They observed that St tended to increase as the shear parameter increased. In addition, the critical Re below which regular vortex shedding was not observed increased as the shear parameter increased.

Much of the work reported here is also reviewed by Sumer & Fredsøe (1997), who also present results from various reports from Sumer and co-workers [(for example, Jensen *et al.* (1990)]. Based on this work, Sumer and Fredsøe suggest that, as G/D decreases, the front stagnation point rotates to a position closer to the plane wall. Similarly, the two flow separation positions move, with the separation point farthest from the wall moving upstream, while the other one moves downstream.

As discussed in this section and summarized in Table 1, there is still considerable uncertainty regarding the flow around a circular cylinder close to plane wall boundary. The objectives of the present paper were to address some of these uncertainties. In particular, the main objective was to use flow visualization and PIV techniques to investigate the apparent cessation of vortex shedding at small values of G/D. Some of the flow visualization results presented here have previously been presented in a highly abridged form by Sumner *et al.* (1999*a*).

2. EXPERIMENTAL APPARATUS AND METHODOLOGY

Two different experimental investigations were performed. Flow visualization and hot-film anemometry experiments were done in a Kempf and Remmers recirculating water tunnel, while particle image velocimetry (PIV) experiments were conducted in a water towing tank. The experimental facilities and techniques have been fully described previously (Sumner 1999; Sumner *et al.* 1999*b*, 2000), and hence only the details pertinent to these specific experiments are presented here.

Experiments in the water tunnel were conducted using a Plexiglas cylinder of 16 mm diameter, D, that spanned the height of the working section (260 mm × 260 mm). The plane-wall boundary, which was positioned in the centre of the water tunnel, was also constructed from Plexiglas; it consisted of a sharp-edged plate of length $20D$, and thickness 6·4 mm, that also spanned the water tunnel height.‡ The combined blockage ratio of the cylinder and plane wall was less than 9%. The cylinder was positioned $10D$ from the leading edge of the plate, see Figure 1.

Flow visualization experiments in the water tunnel were conducted with U in the range 76–89 mm/s, giving $\mathrm{Re} = 1200$–1400. Assuming a laminar boundary layer on the plane wall, the boundary-layer thickness at the cylinder location without the presence of the cylinder, is in the range $\delta = 0{\cdot}46$–$0{\cdot}42D$; however, this was not verified for these experiments.

Flow visualization was achieved using Rhodamine and Fluorescein dyes injected into the flow, either from two ports 120° apart on the cylinder circumference, or from a port $1D$ from the leading edge of the plane-wall boundary. The tunnel was operated below atmospheric pressure, such that the dyes are sucked into the flow from reservoirs; the rate of dye injection was regulated via clamps on the lines connecting the reservoirs to the dye ports. The

‡ The plate was supported at its top and bottom; hence, it was very rigid and did not suffer from vibrations caused by the flow.

visualization was recorded using a JVC Super VHS video camera, and digital images were then acquired from the individual video frames.

Hot-film anemometry experiments were conducted for $86 \leq U \leq 310$ mm/s, giving $1380 \leq \mathrm{Re} \leq 4960$, with exactly the same apparatus as for the flow visualization. A single component hot-film probe was positioned in the wake of the cylinder at either $x/D = 3{\cdot}3$ or 4·8, and at various transverse positions across the cylinder wake from $-0{\cdot}75 < y/D < 2{\cdot}0$; x and y are measured from the centre of the cylinder, as shown in Figure 1. The experimental error in the Strouhal numbers is estimated to be less than 10%; the largest part of this error occurring because of the uncertainty in the velocity measurements.

The PIV experiments were conducted in a water towing tank of 0·76 m × 0·76 m cross-section. The experimental model, consisting of a cylinder of $D = 25{\cdot}4$ mm and a plate of length $20D$ and thickness 6.4 mm, was mounted on a carriage with the plate positioned in the centre of the tunnel, which was towed through the water at a velocity of $U = 75$ mm/s, giving $\mathrm{Re} = 1900$. As for the water tunnel experiments, the cylinder was mounted $10D$ from the leading edge of the plate, and the gap between the cylinder and plate could be adjusted. In this case, the combined blockage ratio of the plane wall and cylinder was a little over 4%. Based on the assumption of a laminar boundary layer on the plate, the boundary-layer thickness at the location of the cylinder, but with the cylinder removed, is estimated to be $\delta = 0{\cdot}36D$.

The water in the towing tank was seeded with nearly neutrally buoyant, irregularly shaped particles of diameters ranging from 100 to 300 μm. The flow was illuminated via a 3–5 mm thick sheet of light from a 5 W argon-ion laser with a mechanical shutter controlled via a pulsed timing generator. The resulting visualization was then recorded using a Dantec FlowGrabber Double Image digital camera, which enabled velocity vectors of the flow to be obtained using the cross-correlation algorithm of Willert & Gharib (1991). Streamline and vorticity plots can then be obtained easily. The size of the interrogation window used in the cross-correlation algorithm effectively limits the minimum size of structure that can be identified using this technique; in these experiments, the interrogation window was $0{\cdot}3 \times 0{\cdot}3D$. As discussed in Sumner *et al.* (1999*a*, *b*), the measurement uncertainty in vorticity is conservatively judged to be approximately 10%.

For each experiment, eight individual sets of data were obtained, with a time interval between successive data-sets of $\Delta t = 0{\cdot}2$ s. Since the camera is fixed, while the cylinder and plate are moving, the field of view is different for each of the data-sets; hence, there is both a temporal and spatial difference between the subsequent plots. For each of the configurations tested, two or three different experiments were conducted to ensure that the results were repeatable. Only one typical set of experimental data is presented here, and for the sake of brevity only some of the eight sets of vorticity data are shown, these being chosen to be most representative of the flow for this configuration.

An example of the vorticity data is shown in Figure 3(a–d) for $G/D = 0{\cdot}125$ (to be discussed completely in the next section). Vorticity contours are presented, in nondimensional form as $\omega D/U$; the minimum level of nondimensional vorticity is 1.0, and the interval between contours is 1.0. The figure caption gives the time interval, Δt, between when each specific data-set was measured and the first of the eight data-sets arbitrarily set at $\Delta t = 0$. Also presented in the figure caption, for each of the data-sets, is the ratio $\Delta t/T_s$, where T_s is the period of vortex shedding calculated assuming a Strouhal number of 0·2. This should not be interpreted to mean that $\mathrm{St} = 0{\cdot}2$ for all cases; indeed for some values of G/D, there is no bulk periodicity of the wake at all. However, as shown subsequently in this paper, $\mathrm{St} = 0{\cdot}2$ represents an approximate average value of the Strouhal numbers over the range of G/D investigated. Hence, using this value of St gives an indication of the relative position of the PIV images in an "average" period of vortex shedding.

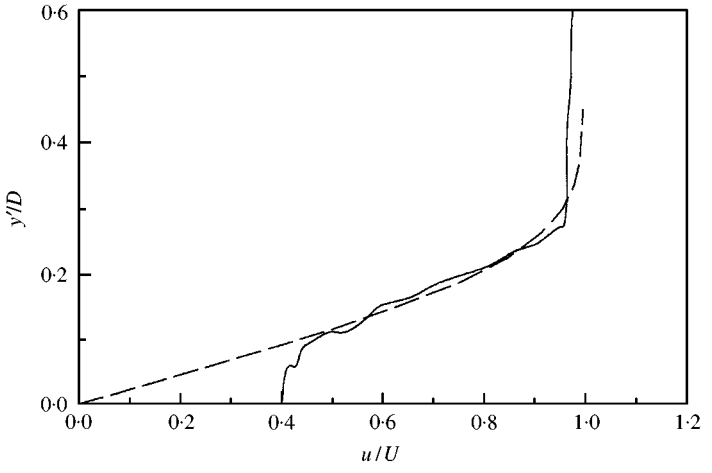

Figure 2. Velocity profile on the flat plate 10D from its leading edge for a towing velocity of 75 mm/s: ——, measurements using PIV; – – – –, theoretical Blasius profile.

3. RESULTS

Initially, experiments were conducted in both facilities to verify the validity of the visualization/measurement schemes. In the water tunnel, flow visualization and measurements of the wake frequency were carried out for an isolated circular cylinder. For $1450 \leq \mathrm{Re} \leq 4100$, a Strouhal number of $\mathrm{St} = 0{\cdot}21$ ($\pm 0{\cdot}01$) was obtained, which is consistent with previously published results (Zdravkovich 1997). To verify the PIV technique, experiments were conducted with the flat plate alone towed through the water. Having obtained the velocity distribution in the flow adjacent to the plate, velocity profiles in the boundary layer were obtained. A typical example at 10D from the leading edge of the plate is shown in Figure 2. Also shown in this figure is the theoretical Blasius profile expected for a laminar boundary layer at this position. Except for regions very close to the wall ($y'/D \leq 0{\cdot}08$ approximately), there is reasonably good agreement between the measured and theoretical profiles. This gives the authors some confidence in both the PIV technique and in the alignment of the plate. However, the poor agreement between the expected boundary-layer profile and the measured results close to the wall is indicative of the difficulties encountered in using the PIV technique in these regions; the main reason for this being the difficulty in obtaining good quality images of particles near the wall because of its shadowing effect when viewed from below. Further details of these verification experiments, as well as other results presented here, are given in Smith (1998) for the water tunnel results, and Leong (1999) for the PIV results; in addition, verification of the experimental procedure is also provided by Sumner (1999) and Sumner *et al.* (1999*b*, 2000).

Returning now to the main objective of this paper, the flow around a cylinder close to a plane wall, it is convenient to discuss the results obtained in four distinct regions, ranging from very small gap ratios, to large gap ratios.

3.1. Very Small Gap Ratios ($G/D = 0$ and $0{\cdot}125$)

Flow visualization at $G/D = 0{\cdot}125$ for $\mathrm{Re} = 1200$–1400, see Figure 3(e), shows evidence of what at first appears to be vortex shedding from the outer shear-layer of the cylinder. This is supported by the PIV results, presented in the form of vorticity contours, shown in

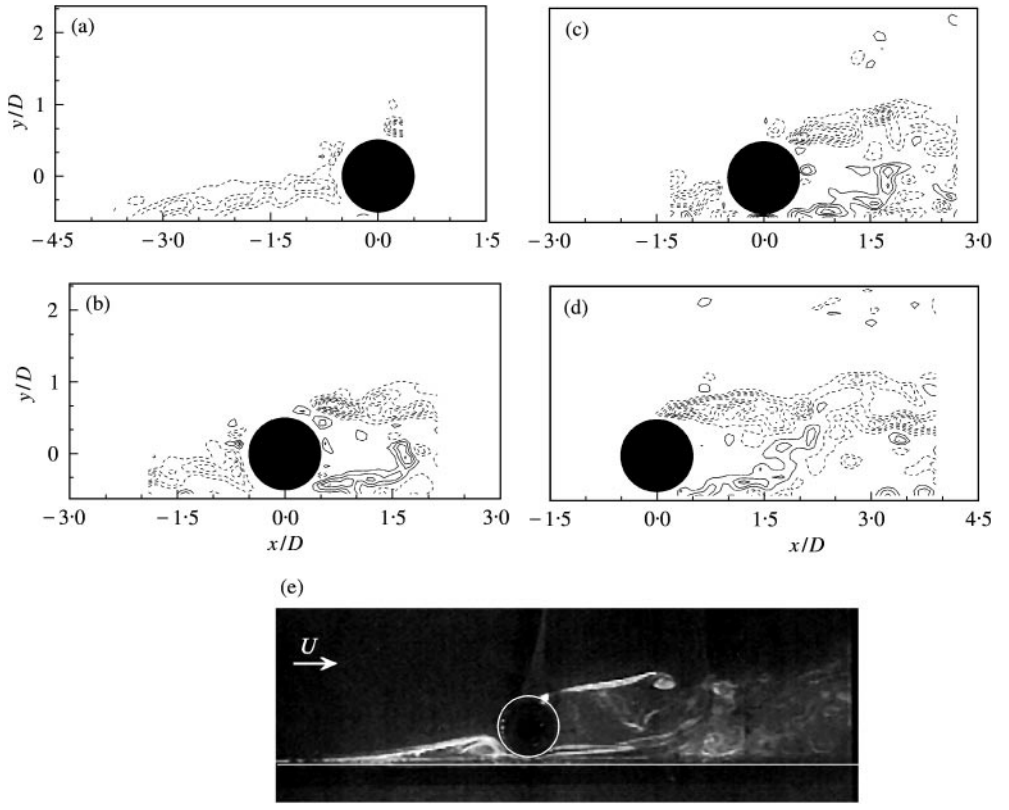

Figure 3. Flow visualization and PIV results for $G/D = 0{\cdot}125$: (a)–(d) PIV vorticity data for Re = 1900; (e) flow visualization for Re = 1200–1400. (a) $\Delta t = 0$, $\Delta t/T_s = 0$; (b) $\Delta t = 0{\cdot}6$ s, $\Delta t/T_s = 0{\cdot}36$; (c) $\Delta t = 0{\cdot}8$ s, $\Delta t/T_s = 0{\cdot}48$; (d) $\Delta t = 1{\cdot}2$ s, $\Delta t/T_s = 0{\cdot}72$; (—— positive, clockwise vorticity; – – negative, counter-clockwise vorticity).

Figure 3(c, d) for a slightly higher Reynolds number of Re = 1900, which indicate that the outer shear-layer has much higher vorticity than the inner one. However, the outer shear-layer extends away from the cylinder and does not roll up to form a regular vortex, as shown in Figure 3(d, e).

Both the flow visualization and PIV results indicate the presence of a separation bubble upstream of the cylinder, followed by reattachment of the flow to the wall as it passes through the gap. However, the video recording of the flow visualization seems to suggest that at regular intervals, the flow ceases to pass through the gap and begins to recirculate in the upstream separation bubble. Downstream of the cylinder, as shown in Figure 3(c, e), the flow appears to separate once again as the inner shear-layer is deflected away from the wall, producing a large region of separated flow. It is also evident that, for this value of G/D, the gap flow between the cylinder and wall is extremely weak.

Although the flow visualization suggests that vortex shedding does not exist, there is a reasonably strong periodic component to the velocity signal measured in the cylinder wake; almost certainly, this is associated with the shear-layer shed from the outside surface of the cylinder. The spectral analysis of this velocity signal, at $G/D = 0{\cdot}125$, indicated that for Re < 2200, the Strouhal number associated with this periodicity is very dependent on Re. For example, Figure 4 shows the wake spectra measured at three different Re. At Re = 1380, see Figure 4(a), the dominant wake frequency is 1.9 Hz, giving St = 0·35; there is

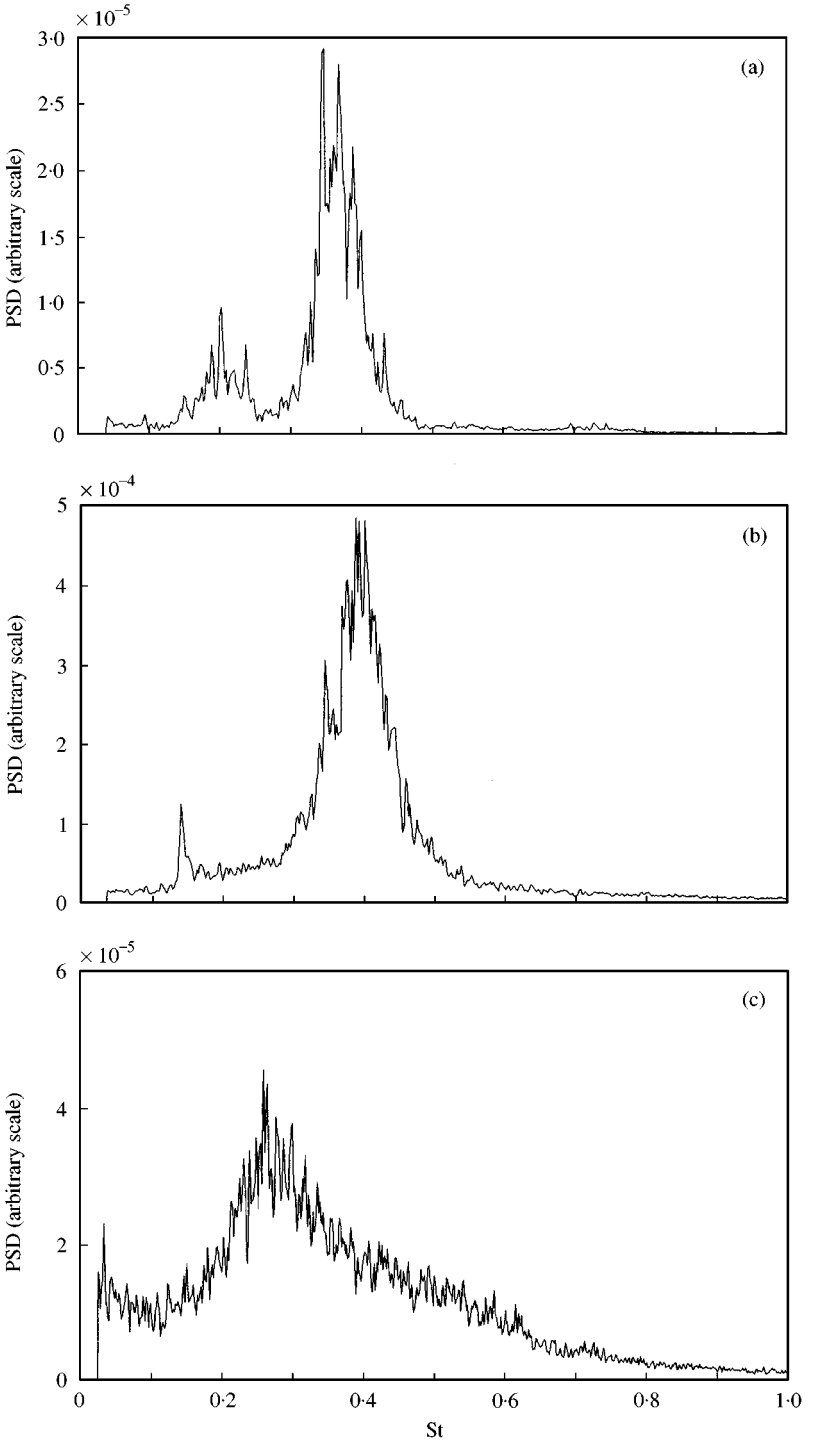

Figure 4. Power spectra of wake velocity for $G/D = 0{\cdot}125$, at location $x/D = 3{\cdot}3$, $y/D = 1{\cdot}5$: (a) Re = 1380 ($U = 86$ mm/s); (b) Re = 1550 ($U = 97$ mm/s); (c) Re = 2210 ($U = 138$ mm/s).

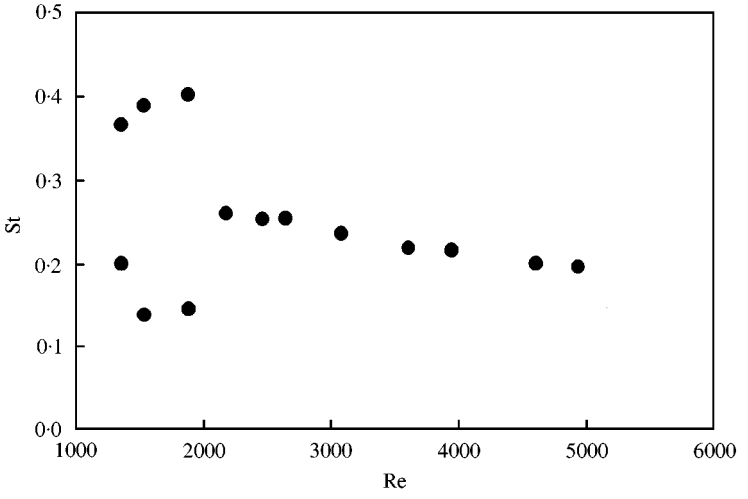

Figure 5. Variation of dominant wake Strouhal number for $G/D = 0{\cdot}125$, at $x/D = 3{\cdot}3$ and $y/D = 1{\cdot}5$, as a function of Re.

also a less prominent peak at 1·14 Hz, giving St = 0·21. As Reynolds number is increased to 1550 the dominant wake peak leads to St = 0·40, see Figure 4(b); similarly, at Re = 1900 (not shown here), St = 0·40 is obtained. However, a further increase in Reynolds number to Re = 2220 leads to St = 0·26; see Figure 4(c). Increasing the Reynolds number beyond this value produces a much more gradual change in St with Re, as shown in Figure 5.

Similar values of St were obtained at the other wake positions for which hot-film measurements were made. However, at some wake positions no dominant wake frequency could be detected; this illustrates some of the difficulties in using spectral analysis of the wake when attempting to determine whether or not a periodicity is present.

No water tunnel experiments were conducted with the cylinder touching the wall, $G/D = 0{\cdot}0$; however, the PIV results, shown in Figure 6, are very similar to those obtained with $G/D = 0{\cdot}125$ (Figure 3). In particular, there is a region of separated flow upstream of the cylinder. The only significant difference between the two sets of results is that for $G/D = 0{\cdot}0$ there is obviously no gap flow, and hence, no shear-layer is shed from the inside surface of the cylinder. However, there *is* a shear-layer, with reasonably strong vorticity, shed from the outer cylinder surface. This shear-layer diverges from the wall as it moves downstream, but shows no indication of curling up to form a vortex.

3.2. Small Gap Ratios ($G/D = 0{\cdot}25$ and $0{\cdot}375$)

The flow behaviour in this region is also characterized by a separation region upstream of the cylinder, as can be seen from both the flow visualization and vorticity fields shown in Figure 7 for $G/D = 0{\cdot}25$. However, by comparing Figures 3 and 7 (particularly the flow visualization images) it is apparent that for $G/D = 0{\cdot}25$, the size of this separation region is considerably smaller than for the "very small gap ratios" of Section 3.1. Furthermore, the size of the separation region decreases as G/D is increased. As the flow accelerates through the gap between the cylinder and wall, it reattaches on the wall. There is then a pairing between the wall shear-layer and that shed from the inner side of the cylinder, the two shear-layers being of opposite sign vorticity. The shear-layer shed from the outer surface of the cylinder does curl up in a periodic manner; however, as for the "very small gap ratios"

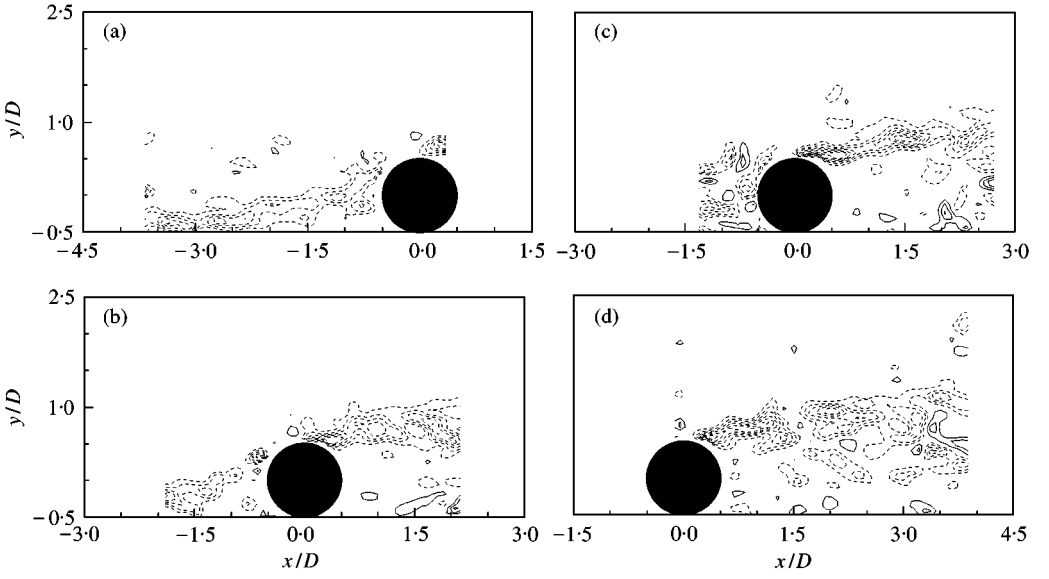

Figure 6. PIV vorticity data for $G/D = 0{\cdot}0$ and Re = 1900: (a) $\Delta t = 0$, $\Delta t/T_s = 0$; (b) $\Delta t = 0{\cdot}6$ s, $\Delta t/T_s = 0{\cdot}36$; (c) $\Delta t = 0{\cdot}8$ s, $\Delta t/T_s = 0{\cdot}48$; (d) $\Delta t = 1{\cdot}2$ s, $\Delta t/T_s = 0{\cdot}72$; (—— positive, clockwise vorticity; – – negative, counter-clockwise vorticity).

this wake periodicity should not be interpreted as vortex shedding. Moreover, the PIV results [Figure 7(c, d)] indicate that the inner shear-layer remains "frozen" for a considerable period of time and, unlike the outer shear-layer, does not roll up. It should be noted that, contrary to the suggestions of Grass *et al.* (1984) and Taniguchi & Miyakoshi (1990), the two shear-layers associated with the wall and the inside of the cylinder, although of different sign vorticity, do not cancel each other out.

A spectral analysis of the wake for $G/D = 0{\cdot}25$ revealed that, in common with the results for "very small gap ratios", St of the dominant wake periodicity is very dependent on Re, see Figure 8(a). For Re ≤ 2600, there is a significant increase in St compared with values obtained for Re > 2600, while for Re > 2600 St is sensibly independent of Re. As shown in Figure 9(a), at Re = 1440 the dominant wake frequency gives St = 0·37; however, there is also a secondary peak at St = 0·19. As the Reynolds number is increased, these two peaks appear to merge into one broad peak, where it is difficult to identify the dominant frequency; see Figure 9(b). A further increase in Reynolds number produces a wake with a very distinct wake frequency; see, for example, Figure 9(c) at Re = 2840.

3.3. Intermediate Gap Ratios ($G/D = 0{\cdot}5$ and 0·75)

In this region, both of the shear-layers shed from the cylinder curl up in an alternating fashion producing a regular vortex shedding pattern, see Figure 10. However, the vortex shedding occurs at a Strouhal number greater than for an isolated circular cylinder. Separation still occurs on the wall upstream of the cylinder, but the size of the separation bubble is now very small. Downstream of the cylinder, separation from the wall occurs in the vicinity of the vortex formation region, and this separation appears to be coupled in a periodic manner with vortex shedding from the cylinder [see Figure 10(d, e)].

Once again, St is very dependent on Re for low Re. For example, as shown in Figure 8(b), for Re ≤ 2500 there is a steady increase in St as Re decreases.

Figure 8. Variation of dominant wake Strouhal number, at $x/D = 3{\cdot}3$ and $y/D = 1{\cdot}5$, as a function of Re: (a) $G/D = 0{\cdot}25$; (b) $G/D = 0{\cdot}5$; (c) $G/D = 1{\cdot}0$.

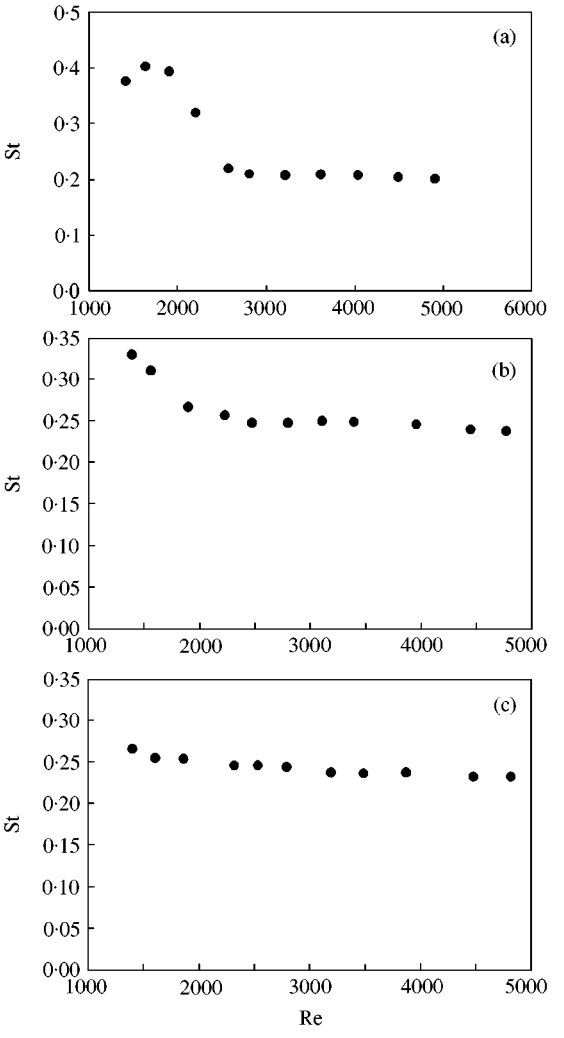

Figure 9. Power spectra of wake velocity for $G/D = 0{\cdot}25$, at location $x/D = 3{\cdot}3$, $y/D = 1{\cdot}5$: (a) Re = 1440 ($U = 90$ mm/s); (b) Re = 2220 ($U = 139$ mm/s); (c) Re = 2840 ($U = 178$ mm/s).

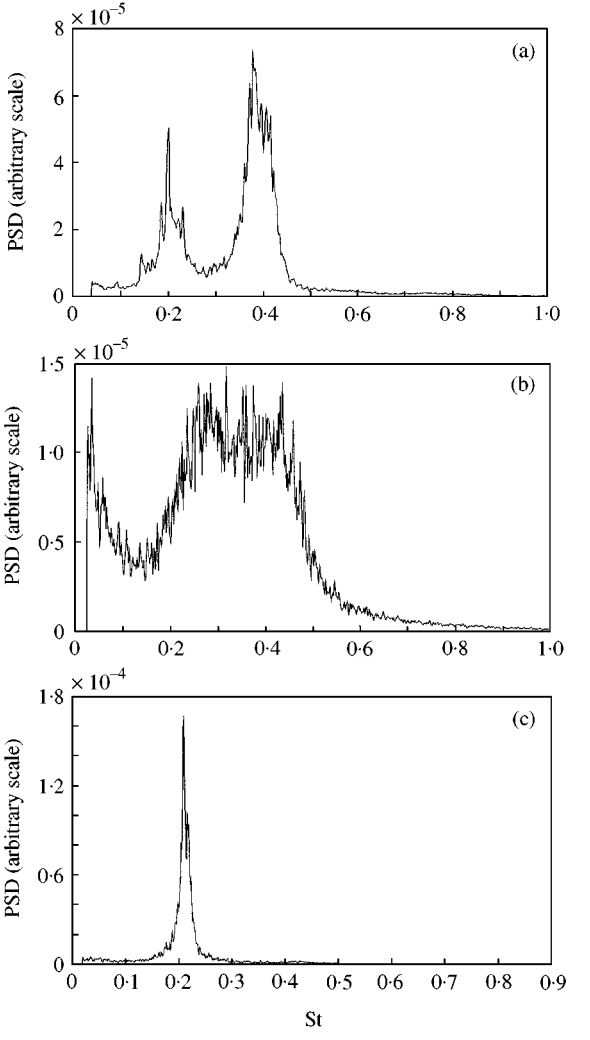

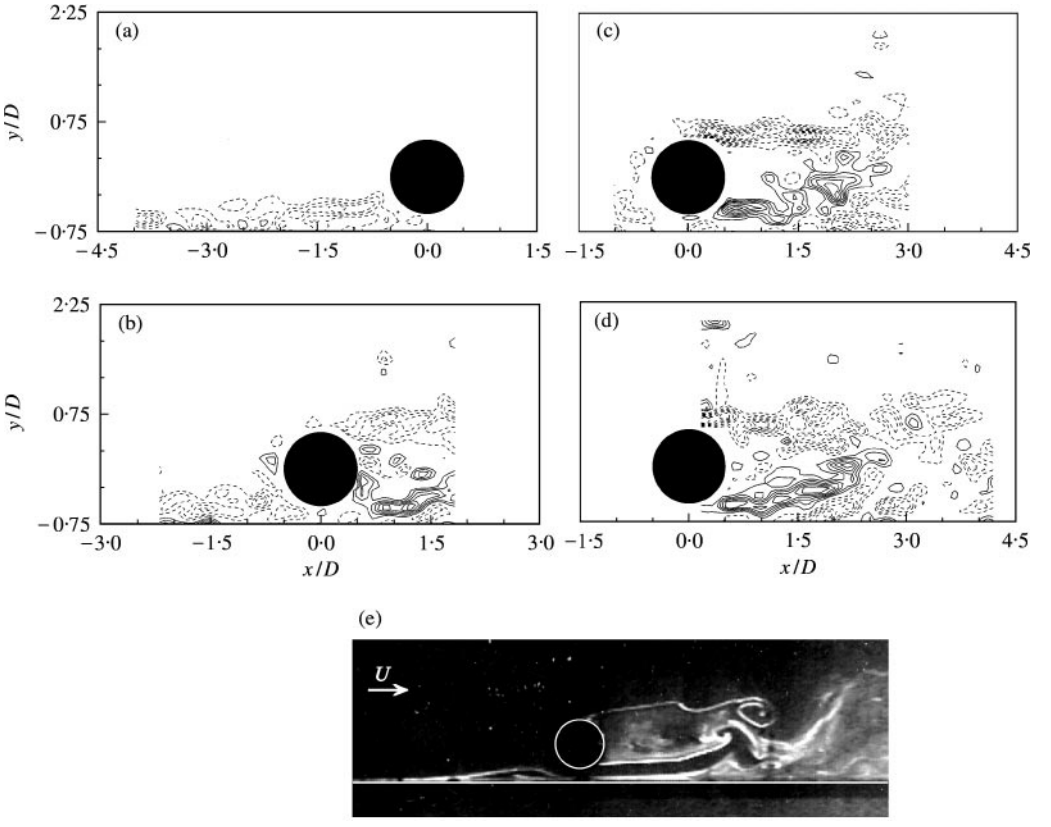

Figure 7. Flow visualization and PIV results for $G/D = 0{\cdot}25$: (a)–(d) PIV vorticity data for $\mathrm{Re} = 1900$; (e) flow visualization for $\mathrm{Re} = 1200$–1400. (a) $\Delta t = 0$, $\Delta t/T_s = 0$; (b) $\Delta t = 0{\cdot}6$ s, $\Delta t/T_s = 0{\cdot}36$; (c) $\Delta t = 1{\cdot}0$ s, $\Delta t/T_s = 0{\cdot}60$; (d) $\Delta t = 1{\cdot}4$ s, $\Delta t/T_s = 0{\cdot}84$; (—— positive, clockwise vorticity; – – negative, counter-clockwise vorticity).

doi:10.1006/jfls.2001.0413

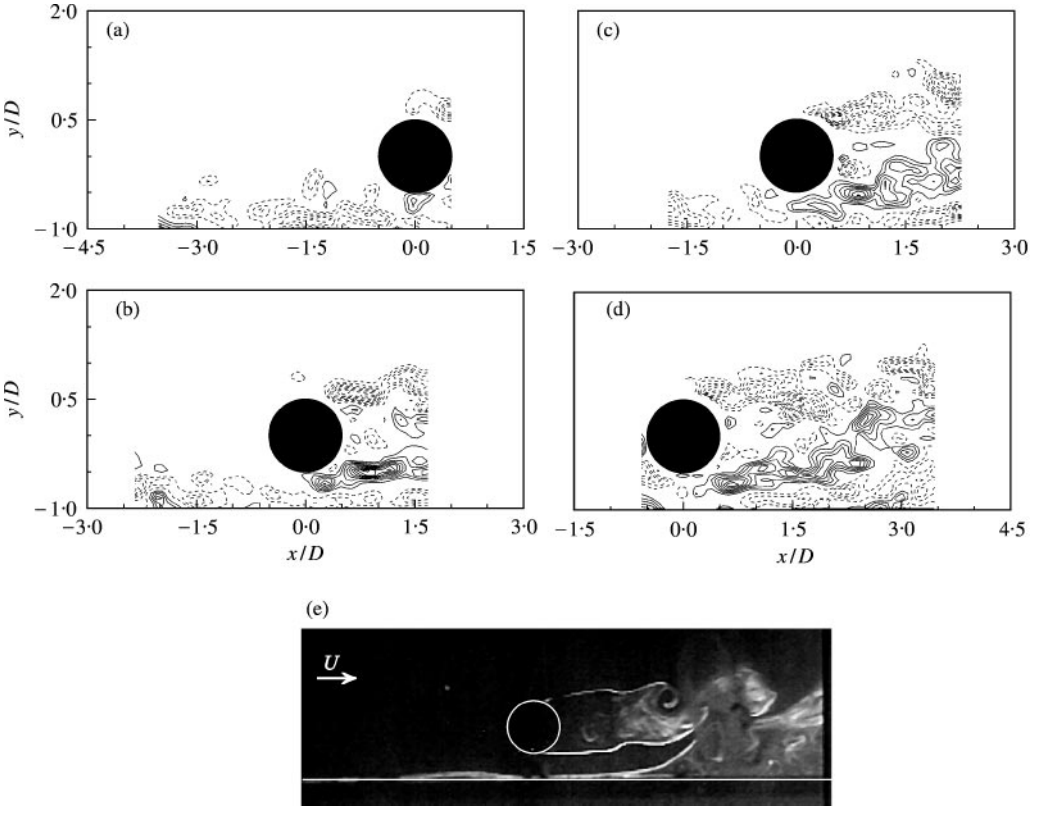

Figure 10. Flow visualization and PIV results for $G/D = 0{\cdot}5$: (a)–(d) PIV vorticity data for Re = 1900; (e) flow visualization for Re = 1200–1400. (a) $\Delta t = 0$, $\Delta t/T_s = 0$; (b) $\Delta t = 0{\cdot}4$ s, $\Delta t/T_s = 0{\cdot}24$; (c) $\Delta t = 0{\cdot}6$ s, $\Delta t/T_s = 0{\cdot}36$; (d) $\Delta t = 1{\cdot}0$ s, $\Delta t/T_s = 0{\cdot}60$; (—— positive, clockwise vorticity; – – negative, counter-clockwise vorticity).

3.4. Large Gap Ratios ($G/D = 1{\cdot}0$, $1{\cdot}5$ and $2{\cdot}0$)

The flow around the cylinder, in this range of G/D, more closely represents that of an isolated circular cylinder (see Figure 11 for $G/D = 1{\cdot}5$). In addition, there is no separation from the wall upstream of the cylinder. However, downstream of the cylinder, alternate vortex shedding from the cylinder affects the wall boundary layer, causing it to separate in a periodic fashion at the same frequency as the vortex shedding. The vorticity induced by the boundary layer separation is in the opposite sense to that shed from the cylinder. This coupling between the vortex shedding from the cylinder and the wall boundary layer decreases as G/D increases, and at $G/D = 2{\cdot}0$, the flow around the cylinder is virtually indistinguishable from that around an isolated cylinder.

For $G/D \geq 1{\cdot}0$, St varies with Re much less than for smaller values of G/D. This is readily apparent by comparing the results of Figure 8(c), for $G/D = 1{\cdot}0$, with those of Figure 8(a, b) for $G/D = 0{\cdot}25$ and $0{\cdot}5$. However, St is still greater than that obtained for an isolated cylinder.

3.5. Strouhal Number Data

A summary of the Strouhal number data obtained from the present experiments for two different Re is presented, as a function of G/D, in Figure 12. It should be noted that while the

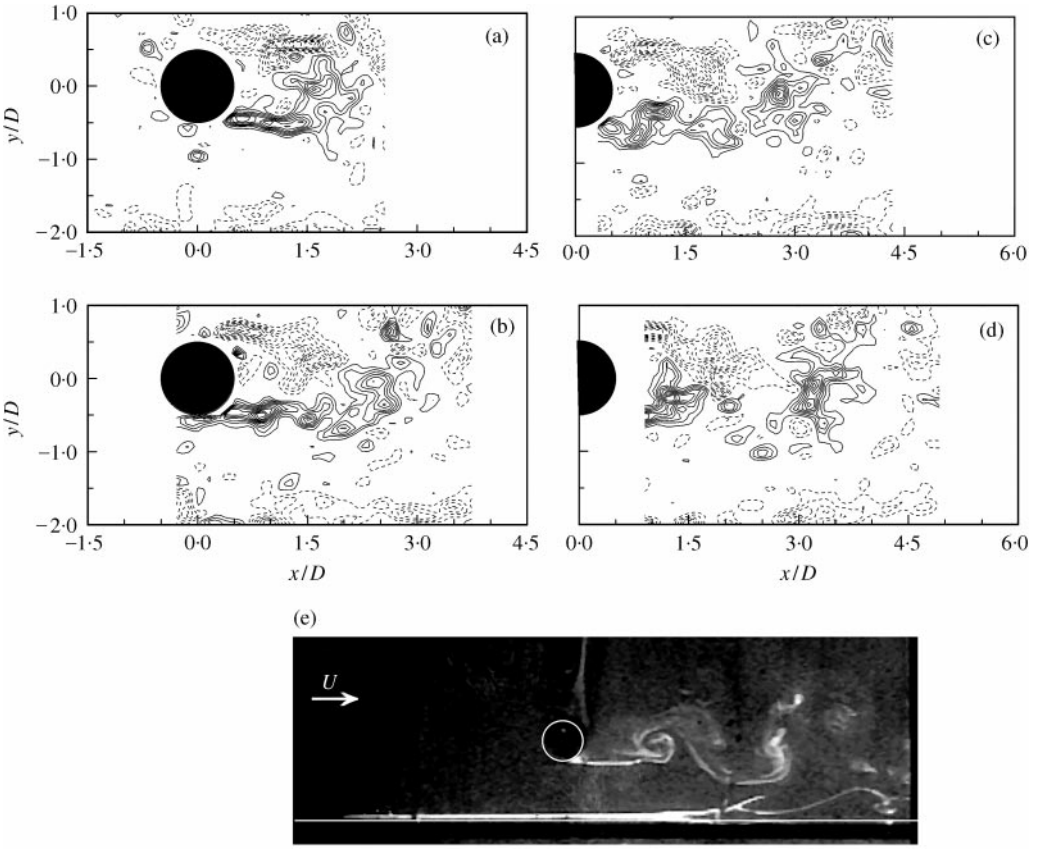

Figure 11. Flow visualization and PIV results for $G/D = 1{\cdot}5$: (a)–(d) PIV vorticity data for Re = 1900; (e) flow visualization for Re = 1200–1400. (a) $\Delta t = 0$, $\Delta t/T_s = 0$; (b) $\Delta t = 0{\cdot}4$ s, $\Delta t/T_s = 0{\cdot}24$; (c) $\Delta t = 0{\cdot}6$ s, $\Delta t/T_s = 0{\cdot}36$; (d) $\Delta t = 0{\cdot}8$ s, $\Delta t/T_s = 0{\cdot}48$; (—— positive, clockwise vorticity; – – negative, counter-clockwise vorticity).

Strouhal numbers for $G/D \geq 0{\cdot}5$ are associated with regular vortex shedding, for $G/D < 0{\cdot}5$ they are more properly associated with the periodicity of the outer shear-layer. Also presented are data obtained by other authors. The present data for Re = 4900 agrees reasonably well with those presented in the previous work. However, the Strouhal numbers measured in the present experiments for Re = 1900 are greater than those reported by other experimenters. This difference is particularly large for $G/D \leq 0{\cdot}25$; however, as previously mentioned, these Strouhal numbers are related to the shear-layer periodicity as opposed to regular vortex shedding.

It is also apparent from Figure 12 that the Strouhal numbers obtained for $\mathrm{Re} \geq 1{\cdot}3 \times 10^4$ (identified by open circles in the figure) show almost no dependence on G/D; this seems to be independent of the boundary layer thickness which is in the range $0{\cdot}1 \leq \delta/D \leq 1{\cdot}64$. Apart from the present results, the only other results which show a significant variation in St with G/D are those of Angrilli *et al.* (1982), for $2860 \leq \mathrm{Re} \leq 7640$. These results, in common with those reported in this paper, show a gradual increase in St as G/D is decreased. Again, this trend seems reasonably independent of boundary-layer thickness, which is in the range $0{\cdot}2 \leq \delta/D \leq 0{\cdot}5$. Hence, it appears that the variation of St with G/D is very dependent on the Reynolds number, and that the Strouhal number is much more sensitive to G/D in the low Reynolds number range of the present experiments.

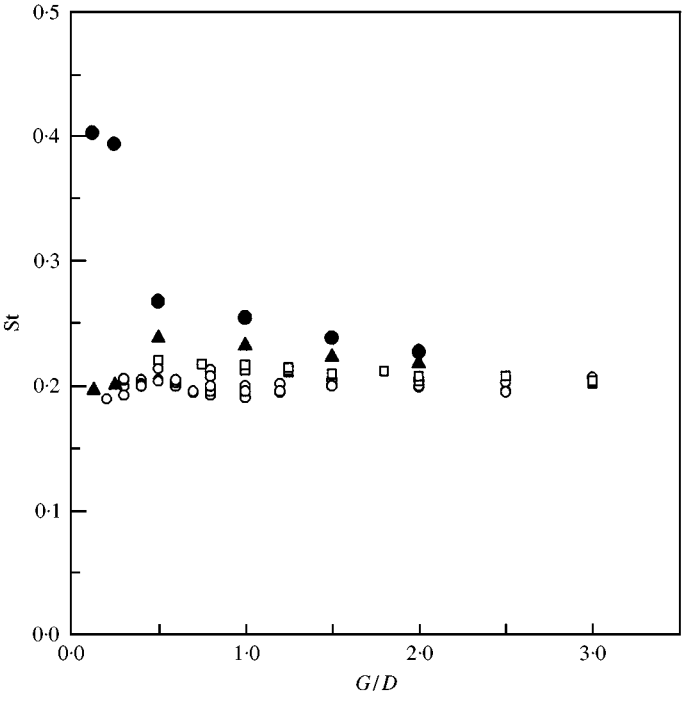

Figure 12. Summary of Strouhal number data: ●, present results, $\delta/D = 0{\cdot}45$, Re = 1900; ▲, present results, $\delta/D = 0{\cdot}45$, Re = 4900; □, Angrilli *et al.* (1982), Re = 2860, 3820, 7640, $\delta/D = 0{\cdot}2$, 0·4, 0·5; ○, Bearman & Zdravkovich (1978), Buresti & Lanciotti (1979), Taniguchi & Miyakoshi (1990) and Lei *et al.* (1999), $1{\cdot}3 \times 10^4 \leq \mathrm{Re} \leq 1{\cdot}4 \times 10^5$, $0{\cdot}1 \leq \delta/D \leq 1{\cdot}64$.

One other significant difference between the present results and those obtained previously is that a wake periodicity frequency is obtained for much smaller values of G/D in the present experiments. However, for $G/D \leq 0{\cdot}25$ ("small" and "very small gap ratios"), the Strouhal number is more properly associated with a periodicity in the outer shear-layer rather than with classical vortex shedding.

4. CONCLUSIONS

Flow visualization, hot film and PIV experiments have been conducted to investigate the flow around a circular cylinder in close proximity to a wall, for Reynolds numbers in the range $1200 \leq \mathrm{Re} \leq 4960$. The results revealed that four distinct regions may be identified for describing the flow the observed flow dynamics.

For very small gap ratios, $G/D \leq 0{\cdot}125$, the gap flow is either suppressed or extremely weak, and no regular vortex shedding occurs downstream of the cylinder. However, it is possible to detect a periodicity in the outer shear-layer. Separation of the boundary layer occurs both upstream and downstream of the cylinder. The size of the upstream separated region decreases as the gap ratio increases. The flow field for small gap ratios, $0{\cdot}25 \leq G/D \leq 0{\cdot}375$, is very similar to that for very small gap ratios, except that there is now a pairing between the inner shear-layer shed from the cylinder and the separated wall boundary layer. Intermediate gap ratios, $0{\cdot}5 \leq G/D \leq 0{\cdot}75$, are characterized by the onset of vortex shedding from the cylinder. In addition, there is a significant reduction in the size of the upstream separation region. For the final region, characterized by the largest gap ratios

considered, $G/D \geq 1{\cdot}0$, there is no separation of the wall boundary layer, either upstream or downstream of the cylinder. In addition, the flow around the cylinder is now essentially the same as the flow around an isolated circular cylinder.

The variation of Strouhal number with gap ratio is very dependent on the Reynolds number. For low Reynolds number flows, $\mathrm{Re} < 2600$, the Strouhal number for $G/D \leq 2{\cdot}0$ is significantly greater than for an isolated circular cylinder. However, for higher Reynolds numbers ($\mathrm{Re} \geq 4000$) St seems to be insensitive to G/D. In addition, in contrast to other studies, there does not seem to be a minimum value of G/D below which periodicities are not detected in the wake. However, for $G/D \leq 0{\cdot}25$ the wake Strouhal number is more properly associated with periodicities in the outer shear-layer from the cylinder, as opposed to classical vortex shedding.

ACKNOWLEDGEMENTS

The authors gratefully acknowledge the financial support of the Natural Sciences and Engineering Research Council (NSERC) of Canada, and Les Fonds pour la Formation de Chercheurs et l'Aide à la Recherche (FCAR) of the province of Québec. The authors would also like to thank Mr S. S.T. Wong who conducted the hot-film experiments.

REFERENCES

ANGRILLI, F., BERGAMASCHI, S. & COSSALTER, V. 1982 Investigation of wall induced modifications to vortex shedding from a circular cylinder. *ASME Journal of Fluids Engineering* **104,** 518–522.

BEARMAN, P. W. & ZDRAVKOVICH, M. M. 1978 Flow around a circular cylinder near a plane boundary. *Journal of Fluid Mechanics* **89,** 33–47.

BURESTI, G. & LANCIOTTI, A. 1979 Vortex shedding from smooth and roughened cylinders in cross-flow near a plane surface. *The Aeronautical Quarterly* **30,** 305–321.

CHENG, M., TSUEI, H. E. & CHOW, K.L. 1994 Experimental study on flow interference phenomena of cylinder/cylinder and cylinder/plane arrangements. In *Flow-Induced Vibration* (ed. M.K. Au-Yang), PVP-Vol. 273, pp. 173–184, New York: ASME.

GRASS, A. J., RAVEN, P. W. J., STUART, R. J. & BRAY, J. A. 1984 The influence of boundary layer velocity gradients and bed proximity on vortex shedding from free spanning pipelines. *Journal of Energy Resources Technology* **106,** 70–78.

JENSEN, B. L., SUMER, B. M., JENSEN, H. R. & FREDSØE, J. 1990 Flow around and forces on a pipeline near a scoured bed in a steady current. *ASME Journal of Offshore Mechanics and Arctic Engineering* **112,** 206–213.

KIYA, M., TAMURA, M. & ARIE, M. 1980 Vortex shedding from a circular cylinder in moderate-Reynolds-number shear flow. *Journal of Fluid Mechanics* **141,** 721–735.

LEI, C., CHENG, L. & KAVANAGH, K. 1999 Re-examination of the effect of a plane boundary on force and vortex shedding of a circular cylinder. *Journal of Wind Engineering and Industrial Aerodynamics* **80,** 263–286.

LEONG, K. 1999 Flow around a circular cylinder near to a plane wall. Undergraduate Honours Thesis, Department of Mechanical Engineering, McGill University.

ROSHKO, A., STEINOLFSON, A. & CHATTOORGOON, V. 1975 Flow forces on a cylinder near a wall or near another cylinder. In *Proceedings of the 2nd National Conference on Wind Engineering Research*, Colorado State University, paper IV–15.

SUMER, B. M. & FREDSØE, J. 1997 *Hydrodynamics around Cylindrical Structures*. Singapore: World Scientific Publishing.

SUMNER, D. 1999 Circular cylinders in cross-flow. Ph.D. Thesis, Department of Mechanical Engineering, McGill University.

SUMNER, D., SMITH, J. G., PRICE, S. J. & PAÏDOUSSIS, M. P. 1999*a* Vortex shedding from a circular cylinder near a plane wall. In *Proceedings of the 17th Canadian Congress of Applied Mechanics* (eds S. ZIADA & D. S. WEAVER) pp. 157–158, McMaster University, Hamilton, Ont., Canada.

SUMNER, D., WONG, S. S. T., PRICE, S. J. & PAÏDOUSSIS, M. P. 1999*b* Fluid behaviour of side-by-side circular cylinders in steady cross-flow. *Journal of Fluids and Structures* **13,** 309–338.

SUMNER, D., PRICE, S. J. & PAÏDOUSSIS, M. P. 2000 Flow-pattern identification for two staggered circular cylinders in cross-flow. *Journal of Fluid Mechanics* **411,** 263–303.

SMITH, J. G. 1998 Flow around a circular cylinder near to a plane wall boundary. Undergraduate Mechanical Laboratory Project, Department of Mechanical Engineering, McGill University.

TANEDA, S. 1965 Experimental investigation of vortex streets. *Journal of the Physical Society of Japan* **20,** 1714–1721.

TANIGUCHI, S. & MIYAKOSHI, K. 1990 Fluctuating fluid forces acting on a circular cylinder and interference with a plane wall. *Experiments in Fluids* **9,** 197–204.

WILLERT, C. E. & GHARIB, M. 1991 Digital particle image velocimetry. *Experiments in Fluids* **10,** 181–193.

ZDRAVKOVICH, M. M. 1977 *Flow around Circular Cylinders. Vol. 1*: *Fundamenatals.* Oxford: Oxford University Press.

ZDRAVKOVICH, M. M. 1980 Intermittent flow separation from flat plate induced by a nearby circular cylinder. In *Proceedings of the 2nd International Symposium on Flow Visualization* (ed. W. Merzkirch), Bochum, West Germany, pp. 265–270.

ZDRAVKOVICH, M. M. 1983 Observation of vortex shedding behind a towed circular cylinder near a wall. In *Proceedings of the 3rd International Symposium on Flow Visualization*, Ann Arbor, Michigan, pp. 391–395.

ZDRAVKOVICH, M. M. 1985 Forces on a circular cylinder near a plane wall. *Applied Ocean Research* **7,** 197–201.